Research Article

EXPERIMENTAL ANALYSES OF EMI NOISE SEPARATOR FOR THE CISPR25 STANDART

Authors: Samet Yalçın(iD), Tuna GÖKSU(iD), Selami KESLER(iD), Okan BİNGÖL(iD)

International Journal of Engineering and Innovative Research

http://dergipark.gov.tr/ijeir

EXPERIMENTAL ANALYSES OF EMI NOISE SEPARATOR FOR THE CISPR25 STANDART

Samet Yalçın[1] , Tuna GÖKSU[1] , Selami KESLER[2] , Okan BİNGÖL[1]

[1]Department of Electrical and Electronics Engineering, Faculty of Technology, Isparta University of Applied Sciences
[2]Department of Electrical and Electronics Engineering, Engineering Faculty, Pamukkale University

*Corresponding Author: sametyalcin@isparta.edu.tr

ABSTRACT: In energy transmission systems, devices must be able to work safely with each other. Therefore, electromagnetic emission and susceptibility of the converting systems are expected to be in a certain range. electromagnetic propagation, especially by radiation and conduction, cannot be neglected in power electronics such as electric vehicle, microgrid, and aerospace technologies. In order to examine and reduce the noise emitted by the devices, the noise should be separated into common mode and difference mode components. In this study, Shou Wang modeling, which is used to separate the noise components into related components, has been examined in order to analyze the noise components within the framework of the CISPR25 standard used for electric vehicles and redesigned. Circuit simulation and design were done and the results were compared. Thanks to these results, it has been seen that the circuit works efficiently up to 90 MHz and gives 8 dB $|S_{11}|$ reflection parameter at the 108MHz threshold level. In addition, the separator circuit was used in a bidirectional DC-DC converter with a known EMI level of 1KW and the noise components obtained were compared with the components of the converter. As a result, it has been seen that the results obtained using the noise separator circuit are almost the same as the real results. In the 18 - 42 MHz range, only the results obtained with the noise separator are up to 8dBuV higher than the real results, other than that the results are exactly the same.

Keywords: Electromagnetic Interference; Interference Anaylses; Noise Separation;Common Mode, Differential Mode, Electrical Vehicles, CISPR25.

1. INTRODUCTION

Importance of power electronics, grid technology and solar power systems is increasing with carbon problems and global warming [1, 2]. Due to the increasing importance of electric vehicles and the importance of smart grid technologies, high-power systems have to work together with sensitive communication technologies and complex control mechanisms. For this reason, electromagnetic interferences emitted by high-power systems appear as factors that must be combated. Understanding and optimizing EMC in switch-mode power supplies is an important problem. The switching action of semiconductor devices causes current pulses at the input and output of power supplies. For CCM operation, PWM converters have rectangular current and voltage waveforms with short rise and fall times as well as high rated di/dt and dv/dt. Therefore, these waveforms exhibit a wide and strong harmonic spectrum. For DCM, PWM converters have triangular current and nearly rectangular voltage waveforms. Cross-conduction of current in transistors connected in series generates very narrow and high current spikes[3].

There are two types of electromagnetic interference (EMI) propagation types. The first of these is emission by radiation, which the EMI source interferes with through the air [4-10], and the second is the emission by transmission, where the source interferes over the line to which it is connected [11, 12]. The form of conducted emission noise is defined by modes in systems. These mode components are divided into two as common mode (CM) and difference mode (DM). CM currents are expressed as the sum of the noise currents flowing from the phase and neutral lines to earth. The reasons for this component are the capacitive effects of MOSFET heatsinks and inductive pulses that may occur on both lines due to switching operations. DM is the noise generated by the difference between the phase and neutral voltages. The main reason for this noise is the interaction between the circuit elements or the circuits themselves [13, 14]. Due to high frequency switching elements, CM noise becomes a much more important problem than DM noise [15].

In order to analyze the EMI of the source of conducted emission, the EMI values are measured with the Line Impedance Stabilization Network (LISN) under the test, over the Spectrum analyzer. When measuring conducted and radiated emission, LISN must be used to prevent noise from the main line and affect the reliability of the test, and to fix the measurement ports at 50 Ω. With such a measurement, the relationship between the device under test (DUT) and CM and DM mode noises is shown in the EMI equivalent circuit in Figure 1.
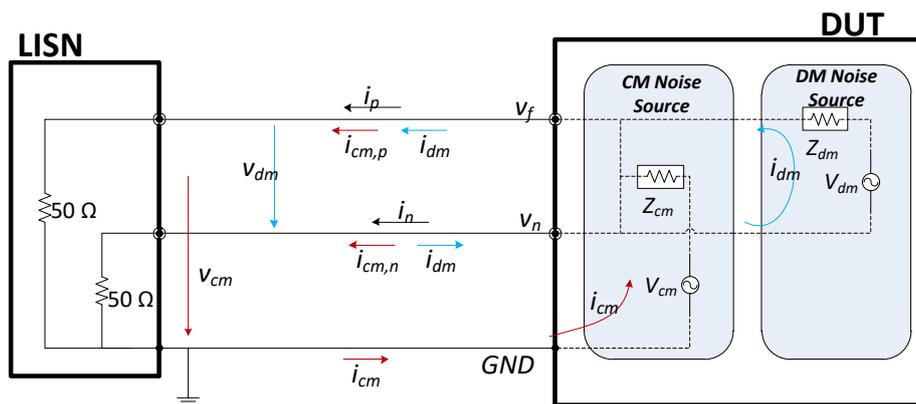
Figure 1: EMI Equivalent Circuit

CM and DM noise modes must be analyzed properly in order to reduce the noise generated in conducted emission at the noise source or propagation path. However, measurements made with LISN do not give any information to the designer about this issue. For that reason, noise modes need to be correctly identified and analyzed for correct suppression [16, 17].

1.1. Differential Mode Noise

DM noise is the noise mode that follows the normal energy path on the lines. The voltage, that is independent of the ground line created by the current flowing from one cable in one direction and from the other cable in the opposite direction, is the difference mode voltage as shown in Figure 2. In other words, the DM noise travels in the same direction as the power in the power line. Thus, interferences in the form of DM flow in the opposite direction on the phase-neutral lines with equal intensity. The main reason for the DM noise is that the circuit components in the device interact with each other and create unwanted voltage differences.
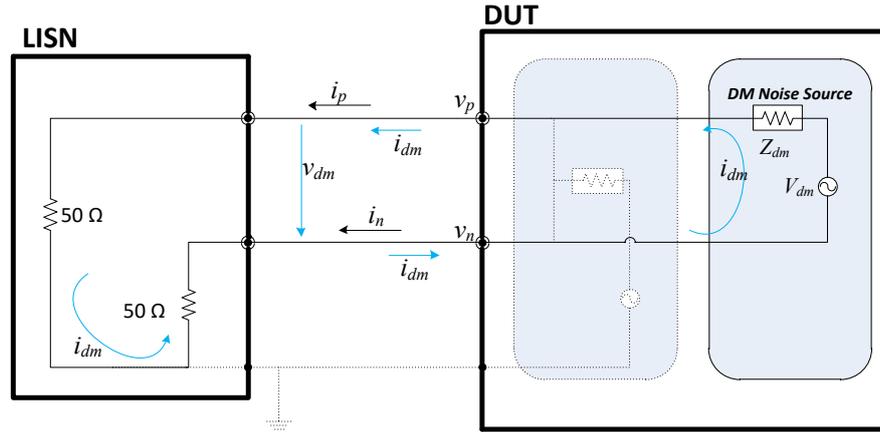
Figure 2: Schematic drawing of EMI DM voltage current

DM current is half of the difference between phase and neutral line currents as given in Eq (1).

$$i_{dm} = \frac{i_p - i_n}{2} \tag{1}$$

The DM voltage is expressed as the difference between the phase and neutral line voltages as given in Eq (2).

$$v_{dm} = v_p - v_n \tag{2}$$

Therefore, the relationship between DM noise voltage and current is defined as follows [11, 18-19]:

$$v_{dm} = v_p - v_n = 50\Omega i_p - 50\Omega i_n = 2 \times 50\Omega \frac{i_p - i_n}{2} = 100\Omega \times i_{dm} \tag{3}$$

1.2.   Common Mode Noise

CM noise voltage is a voltage that affects all power lines in the same direction. This voltage occurs between the lines (phase - neutral) and ground as shown in Figure 3. CM noise usually enters the system through a parasitic capacitance and travels to the ground through the system conductors. The main causes of CM noise are inductive tripping pulses that occur in switching operations in power supplies. In addition, undesirable currents at certain frequencies are sent to the ground by the filter capacitors in the power supplies and the heat sinks in the switching device circuit act as capacitors. This may cause CM noises. Another example of common mode currents is noise from EM pulses caused by nuclear effects and lightning [18].
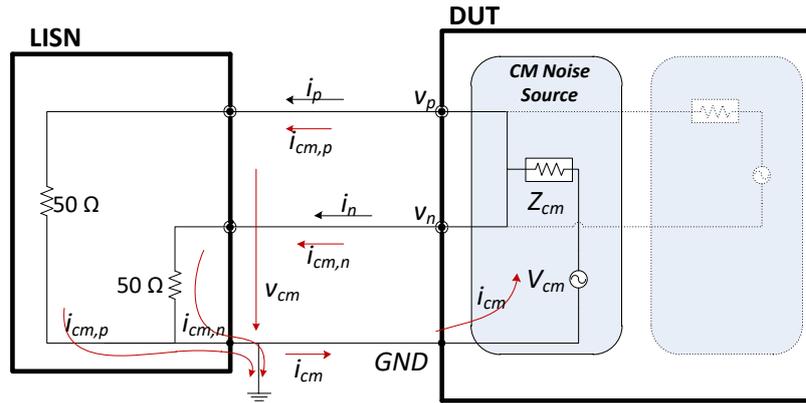
Figure 3: Schematic drawing of EMI CM current

CM currents go from the lines to the ground as shown in Figure 3. It is seen that the CM current is not equal to the phase or neutral line current, but is the sum of the phase and neutral currents as given in Eq (4). The biggest cause of CM currents is parasitic capacitance effects due to circuit structure or ground faults. Because of voltage resulting from this capacitance, CM current flows towards ground. In practice, it is not possible that the impedances of the phase and neutral lines to be equal. For this reason, the common mode current due to the parasitic capacitance cannot be evenly distributed across these lines.

CM currents travel from the lines to the ground as shown in Figure 3. It is understood that the CM current is not equal to the phase or neutral line current, however is the sum of the phase and neutral currents as given in Eq (4). The main cause of CM currents is parasitic capacitance effects due to circuit structure or ground faults. Due to the voltage resulting from this capacitance, CM current flows toward the ground. In practice, it is not possible that the impedances of the phase and neutral lines to be equal. For this reason, the common mode current due to the parasitic capacitance cannot be evenly distributed across these lines.

$$i_{cm} = i_p + i_n \tag{4}$$

In terms of CM noise, the noise presents in the phase and in the neutral line is the same with respect to ground line. Therefore, the CM noise voltage is the arithmetic mean of the phase and neutral voltage as shown in Eq (5). Thus, since one end of the LISN circuit will be terminated with a 50 Ω EMI receiver and the other end with a 50 Ω terminating resistor, the relationship between CM current and voltage will be as shown in Eq (6) [19].

$$v_{cm} = \frac{v_p + v_n}{2} \tag{5}$$

$$v_{cm} = \frac{v_p + v_n}{2} = \frac{50\Omega \times i_p + 50\Omega \times i_n}{2} = \frac{50\Omega}{2}\left(i_p + i_n\right) = 25\Omega \times i_{cm} \tag{6}$$

1.3. Electromagnetic Noise Separator

Determining the levels of the CM and DM noise components in switched-mode power supplies is important to reduce EMI. These components can be evaluated via the EMI receiver. In order to analyze the noise components on the receiver, the noise components must be separated.

Five methods are given in the literature for tests to be carried out on noise voltage measurement. These methods are listed as Paul-Hardin circuit, power combiner, Negal circuit, Caponet circuit, and Shou Wang circuit.

The sum or difference of two input ports from a single output port can be analyzed with the noise separator designed by C. Paul and K. Hardin [20], which is the oldest built using a wideband transformer. However, input impedance of the circuit depends on voltage. This situation creates a great disadvantage for the design.

In another circuit structure designed by Guo [21], the sum or difference of the two input ports is transferred to the output port with the help of phase difference. The results of the design show that the transmission and suppression ratios are very successful. However, in the related article, the (power combiner) equivalent circuit is given as a sum of lines, and the circuit is more complex as it is designed within the subject of microwave engineering.

Another circuit structure was proposed by A. Nagel [22]. This structure is the first transformer-based circuit to deal with the input impedance problem. However, although the CM and DM resistors provide the desired 25 and 100 Ω values as expected, the expected values decrease due to the capacitive noises occurring between the primer and seconder windings of the T1 transformer.
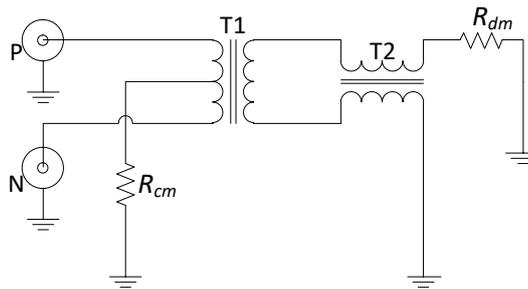
Figure 4: Nagel EMI Separator

Another transformer-based proposal was proposed by C. Caponet and F. Profumo in 2001 and 2002 [23, 24]. However, testing of the proposed circuit is done by measuring the input of the other port, considering that one port input is terminated with a 50 Ω source impedance. This measurement is inaccurate because the source impedance may not be 50 Ω in practice and the terminated port may affect the designed port impedance [25]

Shou Wang developed a proposal with an improved version of Nagel's circuit in 2005 [25]. In the circuit shown in Figure 4, parasitic capacitances between the windings are prevented by not using the second winding in T1.
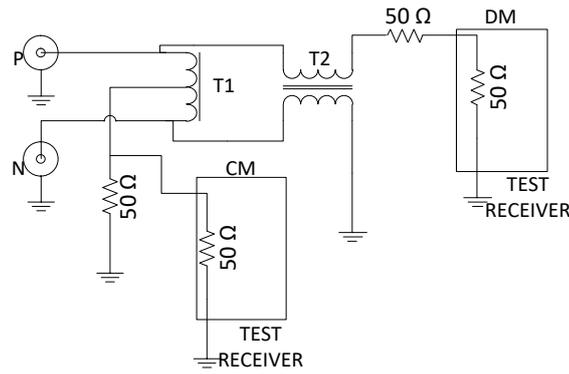
Figure 5: Shou Wang EMI Separator

Kostov's research on methods of separating conducted and radiated emission components [26] reported that Shou Wang's transformer-based noise separator is the method that gives the best results as a passive circuit after the current probe.

EMI receivers have a 50 Ω terminal load. Therefore, the noise separator circuits must also be terminated with 50 Ω. In this way, one line of the noise separator is terminated with an EMI receiver at 50 Ω, while the other line is terminated with 50 Ω so that it can be of the same value. The noise separator circuit was originally designed for use in the 150 kHz – 30 MHz range for CISPR 16. However, there is no noise separator trial performed within the bandwidth of the CISPR 25 standard in the literature .In this study, since the analysis bandwidth is in the range of 150 kHz – 108 MHz, the capability of microwave transformers to be used in circuit design at this level is analyzed and the actual measurement results are shown. In section II, the noise separator has been decided is explained and design with schematic, PCB and actual design. In section III, the result of the design is presented and compared with the calculated CM noise. Then the deviation between the calculated CM noise with the CM noise received via the noise separator is analyzed mathematical deviation methods. Finally, in section IV, the results of measurements are evaluated and it is decided that this noise separator can be used for analyzing CM noise of any circuit.

2. NOISE SEPARATOR DESIGN

For the design of Shou Wang's circuit, the design is carried out on the KiCad program as given in Figure 6. Paying attention to Figure 6(a), it can be seen that Eq (3) and Eq (6) are correctly applied by making the CM port in parallel with a 50 Ω resistor and the DM port in series with a 50 Ω resistor.
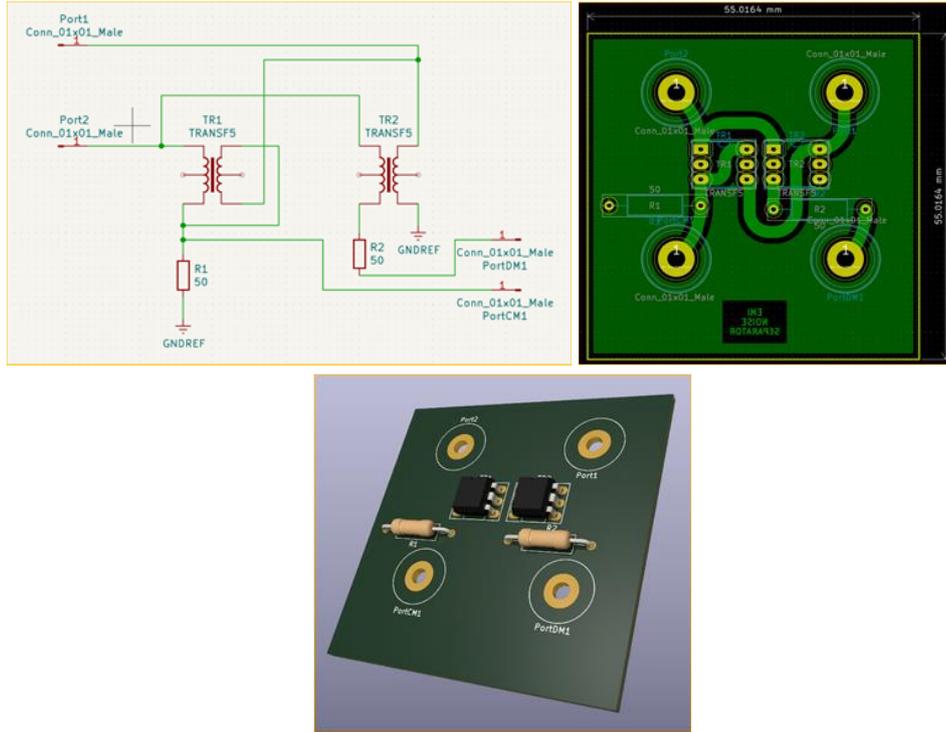
Figure 6: Noise Separator Design

Coilcraft brand wb1010 model broadband RF transformers and N type connectors are used to design the noise separation circuit. The designed circuit is fabricated for experimental analysis as shown in Figure 7.
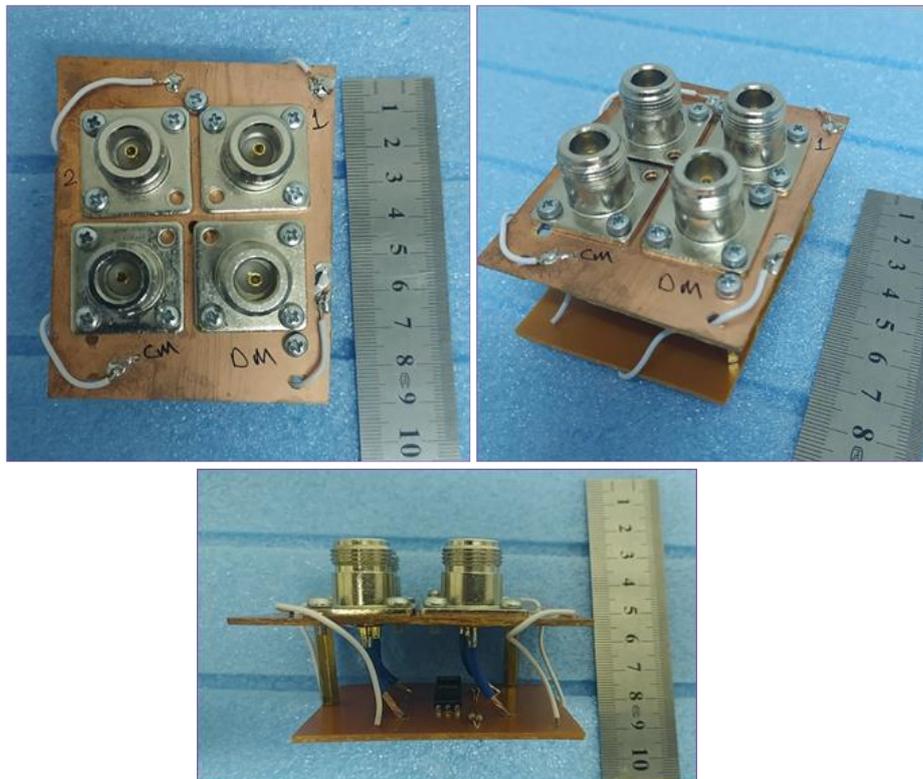
Figure 7: Noise Separator

3. EXPERIMENTAL RESULTS

In order to examine the transmission and reflection ratios of the circuit, the scattering parameter (S-parameter) is examined. Measurements are made by Keysight N9912A Fieldfox Network Analyzer. Figure 8 shows the S-parameter graph. Here, $|S_{11}|$ and $|S_{21}|$ are the reflected wave, and S_{31} and S_{41} are the transmitted wave. The graphics are perfectly compatible with Shou Wang's circuit up to 30 MHz. However, no measurements were found in the literature above 30 MHz. When the circuit is examined with a bandwidth of 150 kHz to 108MHz, it is seen that the transmission and reflection of the circuit approach each other towards the end. When the result in Figure 8, because of the parasitic equivalent parallel capacitor (EPC) of the RF transformer, measurement accuracy is decreasing. But when we examine Figure 10, it is seen that the noise separator can give the actual results.
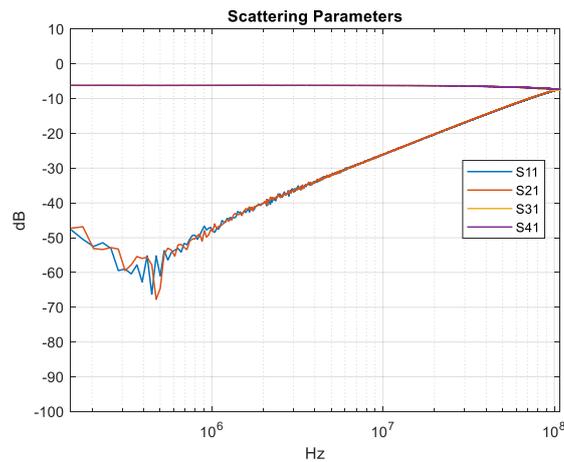
Figure 8: Noise Separator Scattering Parameters

The noise separator circuit, whose scattering parameters were examined, was then used in the real test environment. First, a sample DUT circuit was tested in a laboratory environment established in accordance with CISPR25 standards. This test environment was created as shown in Figure 9. With the help of LISN shown in Figure 9(b), the phase and neutral noise values of the circuit were taken with the Tektronix RSA5126B Spectrum analyzer shown in Figure 9(c), and CM mode and DM mode noise voltages were calculated by applying Eq (2) and Eq(5). Then, the designed noise separator circuit is connected to the LISN port1 and port2 outputs and the CM noise value is taken from the spectrum analyzer.

Figure 9: Conducted Emission Lab Test Bench, LISN and Spectrum Analyzer

The comparison of the calculated CM noise with the CM noise received by the noise separator is shown in figure 10. It is seen that the graphs obtained are almost exactly the same, only the separator measures higher noise in the 18-40 MHz range. But this is not preventing the determination of the EMI values that need to be suppressed.
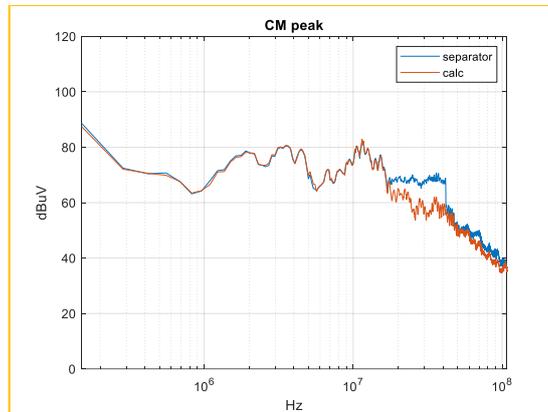
Figure 10: Comparison of CM Noise Separator Result and Calculated CM Noise Result

Deviation in the graphs given in Figure 10 is analyzed mathematically for comparison of the obtained results correctly. Root Mean Square Error (RMSE) and Mean Absolute Deviation (MAD) methods [27, 28] are used to make the comparison.

The RMSE is generally given as

$$RMSE = \sqrt{\frac{1}{n}\sum_{t=1}^{n}(A_t - B_t)^2} \qquad (7)$$

where A_t and B_t are the noise values measured and calculated with the noise separator at each frequency value, respectively. *n* is the sum of the points received in the frequency base between 150 kHz and 108 MHz.

The MAD method generally calculates the static distribution. The terms used in the equation for the MAD method, whose formula is explained below, are the same as those for the RMSE method.

$$MAD = \frac{1}{n}\sum_{t=1}|A_t - B_t| \tag{7}$$

The deviation rates of the noise graphs, whose graphs are given in Figure 10, are calculated by RMSE and MAD methods. As a result of the calculation, the deviation between the graphs was 9.44% according to the RMSE method and 6.83% according to the MAD method

4. CONCLUSION

For successful suppression of EMI, it is essential to analyze and separate the interference into CM and DM components. In order to examine high-power electronic systems, especially used in electric vehicles, within CISPR 25, the noise components must be known. Separation of interference can be done by some methods. In this study, noise separation methods are discussed and the most suitable method is selected.

A noise separator circuit designed in accordance with the chosen method has been designed in the KICAD program by making certain changes. After performing the circuit, the scattering parameters of the noise separator circuit were analyzed with the help of vector network analyzer and the S_{11}-S_{41} parameters were examined in the range of 150kHz – 108MHz. It has been analyzed that the reflection parameter of the circuit increases as the frequency increases. However, the noise separator is also tested with a 1 kW DC-DC converter which EMI and CM-DM mod values were known. The EMI values are compared with the values obtained with the separator. The deviation between noise values are calculated as 6.83% using MAD method. It is shown that the noise separator circuit works successfully and the separator can be used EMI measurements.

REFERENCES

[1]   M. R. Sancar and A. B. Bayram, "Modeling and Economic Analysis of Greenhouse Top Solar Power Plant with Pvsyst Software," International Journal of Engineering and Innovative Research, vol. 5, no. 1, pp. 48 - 59, 2023.
[2]   M. R. Sancar and M. Altınkaynak, "Comparison of Photovoltaic Systems Designed for Different Roof Types for Isparta Province," European Journal of Science and Technology, pp. 1024-1028, 2021.
[3]   MARIAN K. KAZIMIERCZUK, "Pulse-Width Modulated DC–DC Power Converters", John Wiley & Sons, Ltd, 2016.
[4]   A. Genc, H. Dogan, I. B. Basyigit and S. Helhel, "Heatsink Preselection Chart to Minimize Radiated Emission in Broadband on the PCB," in IEEE Transactions on Electromagnetic Compatibility, vol. 63, no. 2, pp. 419-426, April 2021, doi: 10.1109/TEMC.2020.3019958

[5]   H. Dogan, I. B. Basyigit, A. Genc and S. Helhel, "Parametric Study of the Radiated Emission From the Plate-Fin CPU Heatsink at 2–8 GHz," in IEEE Transactions on Electromagnetic Compatibility, vol. 62, no. 6, pp. 2401-2410, Dec. 2020, doi: 10.1109/TEMC.2020.2980773

[6]   I. B. Basyigit, A. Genc, H. Dogan, S. Helhel, "The effect of fin types of the heatsinks on radiated emission on the printed circuit board at S-C band", Microwave and Optical Technology Letters, Volume 62, Issue 10 p. 3099-3106, 2020.

[7]   H. Dogan, I. B. Basyigit and A. Genc, "Variation of Radiated Emission from Heatsinks on PCB according to Fin Types," 2019 3rd International Symposium on Multidisciplinary Studies and Innovative Technologies (ISMSIT), Ankara, Turkey, 2019, pp. 1-4, doi: 10.1109/ISMSIT.2019.8932797.

[8]   I. B. Basyigit, A. Genc, H. Dogan, F. A. Şenel, S. Helhel, "Deep learning for both broadband prediction of the radiated emission from heatsinks and heatsink optimization", Engineering Science and Technology, an International Journal, Volume 24, Issue 3, 2021, Pages 706-714, https://doi.org/10.1016/j.jestch.2021.01.006.

[9]   A. B. Karaman, A. Kocakusak, A. Genç and S. Helhel, "The Effect of Feeding Point on Electromagnetic Emission Due to Heat Sink," 2019 PhotonIcs & Electromagnetics Research Symposium - Spring (PIERS-Spring), Rome, Italy, 2019, pp. 368-371, doi: 10.1109/PIERS-Spring46901.2019.9017476.

[10]   A. Genç, S. Helhel, "The Comparison of EM Characteristics of the Heatsinks with Equal Base Area Depending on the Various Geometries", 10th International Symposium on Intelligent Manufacturing and Service Systems, Sakarya, Turkiye, 2019.

[11]   S. Maniktala, Switching Power Supplies A - Z, Oxford: Elsevier, 2012.

[12]   S. Yalçın, T. Göksu, S. Kesler and O. Bingöl, "Determination of conducted emi in sic based dual active bridge converter," International Journal of Applied Mathematics Electronics and Computers, pp. 241-244, 2020.

[13]   L. Tihanyi, EMC in Power Electronics, Florida: IEEE Press, 2004.

[14]   R. Ozenbaugh, Emi Filter Design Second Edition, New York: Markel Dekker, Inc., 2001.

[15]   M. Montrose and E. Nakauchi, Testing For EMC Compliance Approaches and Techniques, Canada: A JOHN WILEY & SONS, INC., PUBLICATION, 2004.

[16]   S. Yalçin, Ş. Özen and S. Helhel, "EMI flter design based on the separated electromagnetic interference in switched mode power supplies," Turkish Journal of Electrical Engineering & Computer Sciences, p. 3033 – 3043, 2018.

[17]   P. S. Niklaus, M. M. Antivachis, D. Bortis and J. W. Kolar, "Analysis of the Influence of Measurement Circuit Asymmetries on Three-Phase CM/DM Conducted EMI Separation," IEEE Transactions on Power Electronics, pp. 4066 - 4080, 2021.

[18]   D. Bockelman ve W. Eisenstadt, «Combined Differential and Common-Mode Scattering Parameters: Theory and Simulation,» Microwave Theory and Techniques, IEEE Transactions on, Cilt %1 / %20018-9480 , no. 5035123, pp. 1530 - 1539, 1995.

[19]   K. S. Kostov, S. Schroth, F. Krismer, M. Priecinsky, H. -P. Nee and J. W. Kolar, "The Input Impedance of Common-Mode and Differential-Mode Noise Separators," IEEE Transactions on Industry Applications, pp. 2352 - 2360, 2015.

[20]   C. Paul and K. Hardin, "Diagnosis and reduction of conducted noise emissions," Electromagnetic Compatibility, 1988. Symposium Record., IEEE 1988 International Symposium, 1988.

[21]   T. Guo, D. Chen and F. Lee, "Separation of the common-mode- and differential-mode-conducted EMI noise," Power Electronics, IEEE Transactions, vol. 11 , no. 3, pp. 480 - 488, 1996.

[22]   A. Nagel and R. W. D. Doncker, "Separating Common Mode and Differential Mode Noise in EMI Measurement," European Power Electronics and Drives Journal, pp. 27-30, 2000 .

[23]   M. Caponet, F. Profumo, L. Ferraris, A. Bertoz ve D. Marzella, «Common and differential mode noise separation: comparison of two different approaches,» Power Electronics Specialists Conference, 2001. PESC. 2001 IEEE 32nd Annual, cilt 3 , pp. 1383 - 1388, 2001.

[24]   M. Caponet ve F. Profumo, «Devices for the separation of the common and differential mode noise design and realization,» Applied Power Electronics Conference and Exposition, 2002. APEC 2002. Seventeenth Annual IEEE, cilt 1, no. 8, pp. 100 - 105, 2002.

[25]   S. Wang, F. Lee and W. Odendaal, "Characterization, evaluation, and design of noise Separator for conducted EMI noise diagnosis," Power Electronics, IEEE Transactions, vol. 20 , no. 4, pp. 974 - 982, 2005.

[26]   K. Kostov, Design and Characterization of Single-Phase Power Filters, HELSINKI, 2009.

[27]   A. Mehadi, M. Chowdhury, M. N. M., F. Faisal and M. M. Islam, "A software-based approach in designing a rooftop bifacial PV system for the North Hall of Residence," Clean Energy, p. 403–422, 2021.

[28]   M. R. SANCAR and A. K. YAKUT, "Comparative Analysis of SAM and PVsyst Simulations for a Rooftop Photovoltaic System," International Journal of Engineering and Innovative Research, pp. 60-76, 2022.